

WING DOWNLOAD REDUCTION USING VORTEX TRAPPING PLATES

Jeffrey S. Light and Paul M. Stremel
Aerospace Engineers
NASA Ames Research Center
Moffett Field, California

Alan J. Bilanin
Senior Associate
Continuum Dynamics, Inc.
Princeton, New Jersey

Abstract

A download reduction technique using spanwise plates on the upper and lower wing surfaces has been examined. Experimental and analytical techniques were used to determine the download reduction obtained using this technique. Simple two-dimensional wind tunnel testing confirmed the validity of the technique for reducing two-dimensional airfoil drag. Computations using a two-dimensional Navier-Stokes analysis provided insight into the mechanism causing the drag reduction. Finally, the download reduction technique was tested using a rotor and wing to determine the benefits for a semispan configuration representative of a tilt rotor aircraft.

Introduction

Wing download significantly degrades the hover performance of tiltrotor aircraft. A tiltrotor aircraft loses eight to ten percent of each rotor's thrust from rotor wake interactions with the wing. Techniques to reduce wing download have been explored for several years, with limited success. Two-dimensional wind tunnel tests have examined airfoil drag and drag reduction techniques for airfoils at -90 deg angle of attack (Ref. 1). This is a relatively simple way to examine the two-dimensional airfoil aerodynamics for different configurations. Two-dimensional computational analyses have been developed to predict the drag of airfoils at -90 deg (Refs. 2,3). These two-dimensional approaches (experimental and analytical) provide insight into the flow around a two-dimensional airfoil. However, the flow around a tiltrotor wing in hover is highly three-dimensional. Therefore, accurate analysis of wing download requires three-dimensional techniques (analytical and experimental) to couple the rotor and wing flowfields. A three-dimensional Navier-Stokes analysis has been used to model the rotor/wing configuration and calculate download (Ref. 4). This technique used a simple rotor model and predicted many of the three-dimensional flow characteristics observed in experiments. Despite its qualitative success, three-dimensional analysis requires considerable development before it can be used as a design tool. To investigate the

three-dimensional aspects of wing download, tests using semispan rotor/wing models have been conducted for several configurations (Refs. 5-9). Ultimately, testing on an aircraft provides validation of download reduction techniques, as well as associated design tradeoffs (Ref. 5).

Flow visualization during testing has provided useful information about the flowfield over a tiltrotor wing in hover. The flow over the wing is predominantly chordwise near the wing tip, and predominantly spanwise near the wing root (Ref. 10). The chordwise flow is somewhat representative of two-dimensional flow. Therefore, two-dimensional analysis techniques should provide reasonable drag predictions for the wing tip area. The download over the outer portion of the wing (in the rotor wake) is approximately twice as high as the download near the wing root. Therefore, attempts to decrease the two-dimensional drag of the wing over the outboard sections should produce significant benefits.

One method for reducing drag on bluff bodies uses strakes and plates (Refs. 11,12). This paper examines the ability of spanwise plates on the wing upper and lower surfaces, called Vortex Trapping Plates (VTP), to reduce the wing download. Conceptually, the VTP configuration would reduce the drag by generating vortices in the pockets formed by the plates and the wing surface (Fig. 1). This would streamline the flow around the wing and reduce the drag.

This paper presents results from examining the VTP technique using three methods: two-dimensional wind tunnel testing, two-dimensional, unsteady Navier-Stokes computations, and a small-scale, semispan rotor/wing test. This paper examines the effectiveness of the VTP as a download reduction technique and compares the results from the three methods used to evaluate the VTP configurations. The limitations of each of these methods are also discussed.

Evaluation Methodologies

Wind Tunnel Test

An experiment was conducted by Continuum Dynamics, Inc. in the Princeton University 4- by 5-ft wind tunnel. A thin, symmetrical, constant-chord airfoil model (chord = 8.625 in) was used for this test. The airfoil was

Presented at the American Helicopter Society Aeromechanics Specialists Meeting, January 19-21, 1994. Copyright © 1994 by the American Helicopter Society, Inc. All rights reserved.

installed in the tunnel with an angle of attack of -90 deg, i.e., oncoming flow perpendicular to the airfoil chord. No corrections were made to account for the wing blockage of 13 percent. Test section velocities provided a Reynolds number of 363,000 based on the wing chord. VTP's were mounted on the upper and lower surfaces in an attempt to reduce the overall drag of the airfoil. The airfoil drag was measured by the tunnel balance. Wing surface pressures were not measured during the test. Three principal parameters of the VTP's were varied during the test: plate height, h/c ; offset distance from the airfoil leading or trailing edge, x/c ; and angle of the plate with respect to the chord line, θ . Approximately 60 configurations were tested. The parameters examined in the present investigation, x/c and h/c , are shown in Fig. 2.

Navier-Stokes Analysis

The computational technique used in this investigation calculates the viscous flow about a bluff body (Ref. 3). The method provides for the non-iterative solution of the incompressible Navier-Stokes equations by means of a fully coupled implicit technique. This analysis predicted the two-dimensional drag on an XV-15 airfoil section at -90 deg and provided excellent correlation with experiment (Ref. 13).

For the current investigation, calculations were performed for NACA 0012 and V-22 airfoil sections. The NACA 0012 was chosen as representative of the thin, symmetrical airfoil tested in the Princeton wind tunnel test. The calculations were performed for several VTP configurations with no wing flap deflections. To compare these calculations with wind tunnel results, they were performed at a Reynolds number of 363,000, and a -90 deg angle of attack. The predicted drag will be compared with the wind tunnel results.

The V-22 airfoil calculations included VTP's and wing flap deflections of 0 and 78 deg. These calculations were performed at a Reynolds number of 950,000, and an airfoil angle of attack of -73 deg for comparison with the rotor/wing test. The inflow velocity, and therefore, the Reynolds number, was based on twice the momentum theory value for a rotor thrust coefficient of 0.016 (Refs. 5,9). The angle of attack was determined by combining the -85 deg incidence angle of the wing from the rotor/wing test with an estimated 12 deg average swirl angle (Ref. 14). Predicted drag and surface pressures will be compared with experimental results.

Rotor/Wing Test

A rotor/wing test was conducted at the NASA Ames Outdoor Aerodynamic Research Facility using the hover test rig (HTR). The HTR is a general-purpose testbed for small-scale rotors in hover (Fig. 3). The HTR has a 600 HP

motor capable of rotor speeds up to 2867 RPM. Rotor forces and moments were measured by a set of load cells near the test stand base. A three-bladed rigid hub was used for this test. A V-22 rotor with a 3.5 ft radius (7/38-scale) was tested. The rotor thrust was directed downward, with the wake convected upward toward the wing. Previous testing using this rotor test stand has been documented in Ref. 15.

The wing tested had a V-22 airfoil section with a chord of 1.54 ft and a 31 percent, single-slot flap. Testing was conducted for flap deflections of 0 and 78 deg. The wing and flap had four chordwise rows of 34 static pressure taps on the upper and lower surfaces. Wing pressures at 47 percent of the rotor radius (0.47 R) were used to examine the effects of the VTP's on reducing the section drag. Previous experiments using flow visualization have shown this radial station is in the chordwise flow region of the wing that most closely represents two-dimensional flow (Ref. 8).

The wing was mounted above the rotor using a dual-arm support system that provided for unobstructed flow between the rotor and wing. Each arm of the support system contained a balance for measuring the loads on the wing. The wing was mounted in a V-22 tiltrotor configuration with a -85 deg incidence angle and 3 deg dihedral.

An image plane, mounted from the wing support structure and independent of the wing balances, was used to simulate the flowfield of the second rotor of a tiltrotor aircraft. The image plane was 16 ft wide by 12 ft tall (4.57 R wide by 3.43 R tall), with approximately 10 ft (2.86 R) extending on the rotor side of the wing, as shown in Fig. 3. The image plane was installed to simulate 6 deg of forward wing sweep.

All measurements during the test were acquired for ambient wind speeds at or below 5 knots. Full-scale tip Mach numbers ($M_{tip} = 0.69$) were maintained during testing, and thrust coefficients (C_T) tested ranged from 0.005 to 0.018. Results at a thrust coefficient of 0.016 were used for comparisons with the two-dimensional analysis.

Results

Vortex Trapping Plates on Symmetrical Airfoil

The sixty VTP configurations tested in the wind tunnel test provided a wide range of drag results. The drag ratio (measured drag/baseline drag) ranged from 1.11 to 0.58. Several of the configurations that provided significant results were examined using the Navier-Stokes analysis. The cases examined and the drag ratio for each are shown in Table 1.

The analysis predicts a slightly greater drag reduction than was measured for the VTP configuration using only upper surface plates (Configuration (a)). The flow mechanism leading to the observed drag reduction can be

understood by examining the calculated surface pressure coefficients (Fig. 4). Recirculating vortices form on the upper surface between the VTP and the leading and trailing edges. These vortices decrease the pressure on the upper surface, thereby decreasing the drag. The upper surface plates also increase the pressure on the lower surface of the airfoil, thereby decreasing the drag. Since experimental surface pressures are not available, it is difficult to precisely determine the reason for the discrepancy in drag coefficients for Configuration (a). No corrections were made to the wind tunnel data for blockage or wall effects. It is conceivable that these corrections could significantly alter the drag for the wing configurations tested (Ref. 1). Also, no investigation has been performed to determine the sensitivity of numerical results to grid resolution in the region where the vortices are trapped. The effect of the corrections or grid resolution on the change in drag between any two configurations is unknown.

The analysis predicts an increase in the drag ratio (1.07) for the VTP configuration with two lower surface plates (Configuration (b)). This is in contrast to the slight reduction (0.91) measured in the wind tunnel. The increase in predicted drag is caused by the recirculating vortices formed between the VTP and the leading and trailing edges. These vortices produce a suction on the wing lower surface, which increases the drag (Fig. 5). The lower surface plates do not significantly alter the predicted pressures on the wing upper surface. The reason for the discrepancy between measured and predicted drag ratios is, as mentioned above, conjecture.

With plates on the upper and lower surfaces, Configuration (c), the drag ratio is 0.77 for both the experiment and the analysis. The predicted pressures in Fig. 6 show that the individual effects from the upper surface plates and the lower surface plates are combined for this configuration. The decrease in pressure on the upper surface and the increase in pressure on the lower surface, caused by the upper surface VTP, are evident in the figure. The suction on the lower surface, caused by the lower surface VTP's, is also evident.

Vortex Trapping Plates on V-22 Wing: Flap = 0 deg

Results from the analysis were compared with experimental measurements from the rotor/wing test. Early predictions with the wing angle of attack at -85 deg provided significantly different pressures than those measured. Including the estimated average swirl angle of 12 deg provided much better agreement. Figure 7 shows the influence of angle of attack on the calculations for the V-22 wing. The stagnation pressure shifts forward approximately 15 percent of the chord. This can significantly alter the predicted drag and the drag reduction capabilities of the VTP's. Therefore, when examining download reduction

devices using two-dimensional analysis or testing, it is important to use an appropriate angle of attack.

Comparisons between predicted and measured surface pressures for the baseline V-22 wing with no VTP's and a flap deflection of 0 deg are shown in Fig. 8. The drop in pressure on the wing upper surface at $x/c \approx 0.75$ for the experimental data is the result of not sealing the flap/wing gap for that case. The gap was sealed for all subsequent runs. The experimental and analytical results for the magnitude and location of the maximum pressure on the upper surface correspond reasonably well. However, the analysis predicts a more rapid decrease in pressure toward the leading and trailing edges than was measured experimentally. Too few experimental pressure measurements were obtained near the wing leading edge to show the suction at the leading edge predicted by the analysis. The analysis predicts a significantly lower base pressure than was measured during testing. This difference between the two- and three-dimensional base pressures is consistent with findings from several previous investigations (Refs. 1,3,4,5,6,9). The two-dimensional base pressure is a direct result of the vortices shed from the airfoil. The three-dimensional flowfield for a tiltrotor in hover apparently decreases the effect of the shed vortices on the wing lower surface. This could be caused by three-dimensional flow over the wing or interactions with the rotor tip vortices.

Including upper surface VTP's on the wing results in the pressure distribution shown in Fig. 9. The leading edge plate does not alter the pressure distribution as was seen in Fig. 4. This is caused by the forward shift in the stagnation pressure resulting from the different angle of attack. However, the angle of attack change contributes to a more pronounced pressure drop at the trailing edge VTP than that shown in Fig. 4. The analysis predicts a more significant decrease in pressure on the upper surface than was measured experimentally (Fig. 9). The base pressures are in closer agreement than observed for the baseline wing configuration in Fig. 8. This is because the analysis predicts an increase in the base pressure with the use of the VTP's, while no change is evident from the experimental measurement.

Vortex trapping plates on both the upper and lower surfaces was also examined experimentally and analytically. The analysis again shows a more significant decrease in pressure as a result of the trailing edge VTP (Fig. 10). The analysis also predicts a lower pressure at the wing leading and trailing edges due to the lower surface plates. This contributes to the increased drag relative to Configuration (d). This is not evident for the experimental results, largely because of the low number of pressure measurements obtained on the wing lower surface.

The change in download from the two VTP configurations is shown in Table 2 for the V-22 wing with 0 deg flap. Results for the analysis and rotor/wing test are included. The download ratio is defined as the measured download (or vertical drag) with VTP's installed divided by

the download without VTP's. The analysis and experiment both show a download reduction from the VTP's. The predicted download ratios are somewhat lower than the measured values. This is caused mainly by the discrepancies noted for the base pressures. The closer agreement between the analysis and experiment for Configuration (e) results from the predicted suction on the lower surface between the VTP and the leading and trailing edges.

Vortex Trapping Plates on V-22 Wing: Flap = 78 deg

Deflection of the flap on a tiltrotor wing significantly reduces both the wing area and the drag coefficient, thus reducing the download. The effect of the VTP's on the section download for a V-22 wing with the flap deflected 78 deg was examined analytically and experimentally. The section download ratios for the three configurations examined are summarized in Table 3. The analysis predicts small to modest reductions in download for each configuration. The changes found from the experiment are insignificant for Configurations (f) and (g), and are better than predicted for Configuration (h).

The analysis predicts a small decrease in the download for Configuration (f). This is mainly the result of the increase in pressure on the wing lower surface (Fig. 11). The inability of the analysis to correctly predict the three-dimensional base pressure for previous configurations raises doubts as to the download reduction predicted for this configuration.

The experimental wing pressure measurements for Configuration (f) show an intriguing characteristic (Fig. 12). A region of decreased pressure is evident just aft of the VTP. It appears that a recirculating vortex forms aft of the VTP. However, the expected angle of attack (-73 deg) is not large enough to cause the significant separation required to form the vortex. It is possible that the influence of the rotor tip vortices assists in the formation of the recirculating vortex. The dip in the upper surface pressure was also measured for Configuration (g).

Another interesting result evident when comparing the drag predictions for Configurations (f) and (g) is that the addition of the lower surface VTP improves the download reduction. This is in apparent contrast to the change in download obtained between Configurations (d) and (e). The difference in the calculated download arises from the offset distance (x/c) of the lower surface plate. The lower surface VTP for Configuration (e) is at $x/c = 0.145$. This is far enough from the leading edge to allow a recirculating vortex to form. This decreases the pressure on the lower surface further, thereby increasing the download. The lower surface VTP for Configuration (g) is at $x/c=0.029$. No recirculating vortex forms between the wing and the lower surface VTP (Fig. 13). However, the VTP moves the release point for

the wing shed vortex further from the wing lower surface, thereby increasing the base pressure and decreasing the download.

A significant section download reduction was measured for Configuration (h). The reduction in download is caused by the large decrease in the upper surface pressure aft of the upper surface VTP located at $x/c = 0.61$ (Fig. 14). This is indicative of a recirculating vortex as seen earlier. The analysis also predicts a drop in pressure aft of the VTP (Fig. 15). However, a smaller percentage drag reduction is predicted by the analysis. The difference in the base pressure between the analysis and experiment (Fig. 7) for the baseline wing results in a higher download for the analysis relative to the experiment. The calculated change in drag resulting from the upper surface pressure drop, though it is about the same magnitude as measured, provides a smaller percentage reduction.

Wing Download Reduction

The two-dimensional results provide insight into the process of section download reduction using the VTP's. However, the ultimate goal is to decrease the download on the entire wing. This is a combination of relatively two-dimensional drag at the wing tip and momentum drag (from the fountain) at the wing root. Data from the rotor/wing test indicate the VTP's can provide a reduction in the overall wing download. Figure 16 shows the download to thrust ratio measured for two VTP configurations as well as the baseline wing with flap = 0 deg. The upper surface VTP's provide a 10 to 15 percent reduction in download over a wide range of thrust coefficients. The addition of VTP's on the wing lower surface does not significantly alter the download. The magnitude of download reduction doesn't directly correspond to the results of Table 2. This is expected since the results of Table 2 are two-dimensional and don't account for the drag over the complete wing or the effect of the fountain flow on the download. However, the section download reduction techniques from Table 2 translate to a decrease in wing download.

The download to thrust ratios for the VTP configurations with the wing flap deflected 78 deg are shown in Fig. 17. Modest reductions are obtained for all VTP configurations. Configuration (g) provided the most significant download reduction (7 percent at $C_T = 0.016$). Configuration (g) also provided the largest predicted section download reduction (Table 3). However, Configuration (h), which showed a large measured section download reduction in Table 3, does not provide a large wing download reduction. The measured wing surface pressures from different wing spanwise locations provide insight into this discrepancy. The measured vertical pressure coefficients from the rotor/wing test for Configurations (h) and (g) are shown in Figs. 18 and 19 respectively. The large pressure drop aft of the VTP that is responsible for the section

download reduction is evident for all the spanwise stations in Fig. 18. However, the upper surface pressures at the 0.99 R station in Fig. 18 are twice as high as those for Configuration (g) shown in Fig. 19. This demonstrates how download reduction techniques can benefit the targeted wing location at the expense of other locations.

Conclusions

Vortex Trapping Plates have been examined as a method of reducing tiltrotor wing download. The examination has consisted of two-dimensional wind tunnel testing, analysis using a two-dimensional Navier-Stokes analysis, and three-dimensional testing of a rotor and wing. Comparisons were made between these different techniques and the benefits and drawbacks of each were discussed. Among the findings were:

1. VTP's on the upper and lower surfaces of airfoils at -90 deg angle of attack reduced the drag on the airfoil up to 23 percent in two-dimensional testing.
2. The two-dimensional Navier-Stokes calculations provide insight into the flow around the airfoil. The angle of attack used in the calculations can significantly alter results. Improved correlation of experimental and analytical results will require measurements of rotor wake swirl measurements near the wing location. Also, the base pressure calculations do not agree with measurements from three-dimensional testing.
3. Vortex Trapping Plates reduced the wing download by 7 percent at $C_T = 0.016$ for the V-22 wing with flap = 78 deg. Configurations with the largest predicted two-dimensional drag reductions did not necessarily provide the highest download reduction.
4. The download for a selected wing section can be reduced using two-dimensional techniques, but it may increase the download at another location. Future wing download reduction techniques will need to address this issue.

References

1. Maisel, M. D., Laub, G. H., and McCroskey, W. J., "Aerodynamic Characteristics of Two-Dimensional Wing Configurations at Angles of Attack Near -90 Degrees," NASA TM 88373, Dec. 1986.
2. Raghavan, V., McCroskey, W. J., Van Dalsem, W. R., and Baeder, J. D., "Calculations of the Flow Past Bluff bodies, Including Tilt-Rotor Wing Sections at $\alpha = -90^\circ$," AIAA Paper 90-0032, AIAA Aerospace Sciences Meeting, Reno, NV, Jan. 1990.
3. Stremel, P. M., "Calculation of Unsteady Airfoil Loads with and without Flap Deflection at -90 Degrees Incidence," AIAA Paper 91-3336, AIAA Aircraft Design and Systems Meeting, Baltimore, MD, Sept. 1991.
4. Fejtek, I. G., "Navier-Stokes Flowfield Computation of Wing/Rotor Interaction for a Tilt Rotor Aircraft in Hover," NASA CR 4532, July 1993.
5. Wood, T. L. and Peryea, M. A., "Reduction of Tiltrotor Download," American Helicopter Society 49th Annual Forum, St. Louis, MO, May 1993.
6. Felker, F. F., "Wing Download Results from a Test of a 0.658-Scale V-22 Rotor and Wing," *Journal of the American Helicopter Society*, Vol. 37, No. 4, Oct. 1992.
7. Mc Veigh, M. A., Grauer, W. K., and Paisley, D. J., "Rotor/Airframe Interactions on Tilt Rotor Aircraft," *Journal of the American Helicopter Society*, Vol. 35, No. 3, July 1990.
8. Felker, F. F., and Light, J. S., "Aerodynamic Interactions Between a Rotor and Wing in Hover," *Journal of the American Helicopter Society*, Vol. 33, No. 2, April 1988.
9. Felker, F. F., Signor, D. B., Young, L. A., and Betzina, M. D., "Performance and Loads Data from a Hover Test of a 0.658-Scale V-22 Rotor and Wing," NASA TM 89419, April 1987.
10. Felker, F. F., "A Review of Tilt Rotor Download Research," 14th European Rotorcraft Forum, Milano, Italy, Sept. 1988.
11. Pamadi, B. N., Pereira, C., and Laxmana Gowda, B. H., "Drag Reduction by Strakes of Noncircular Cylinders," *AIAA Journal*, Vol. 26, No. 3, Aug. 1990.
12. Lanser, W. R., Ross, J. C., and Kaufman, A. E., "Aerodynamic Performance of a Drag Reduction Device on a Full-Scale Tractor/Trailer," SAE Aerospace Technology Conference and Exhibition, Long Beach, CA, Sept. 1991.
13. Stremel, P. M., "The Effect of Reynolds Number and Turbulence on Airfoil Aerodynamics at -90 Degrees Incidence," AIAA Paper 93-0206, AIAA Aerospace Sciences Meeting, Reno, NV, Jan. 1993.
14. Johnson, W., *Helicopter Theory*, Princeton University Press, 1980.

15. Swanson, A. A., and Light, J. S., "Shadowgraph Flow Visualization of Isolated Tiltrotor and Rotor/Wing Wakes," American Helicopter Society 48th Annual Forum, Washington D.C., June 1992.



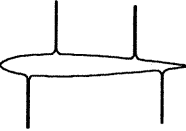
Configuration	Drag Ratio	
	Tunnel	Analysis
a) 	0.78	0.62
b) 	0.91	1.07
c) 	0.77	0.77

Table 1. Symmetrical Wing, $\alpha = -90$ deg.


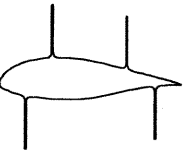
Configuration	Download Ratio	
	R/W Test	Analysis
d) 	0.67	0.59
e) 	0.72	0.68

Table 2. V-22 wing with flap = 0 deg, $\alpha = -73$ deg.

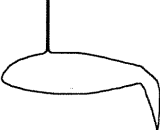
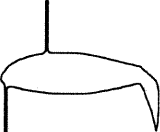
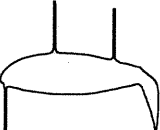
Configuration	Download Ratio	
	R/W Test	Analysis
f) 	1.01	0.92
g) 	1.01	0.87
h) 	0.76	0.96

Table 3. V-22 wing with flap = 78 deg, $\alpha = -73$ deg.

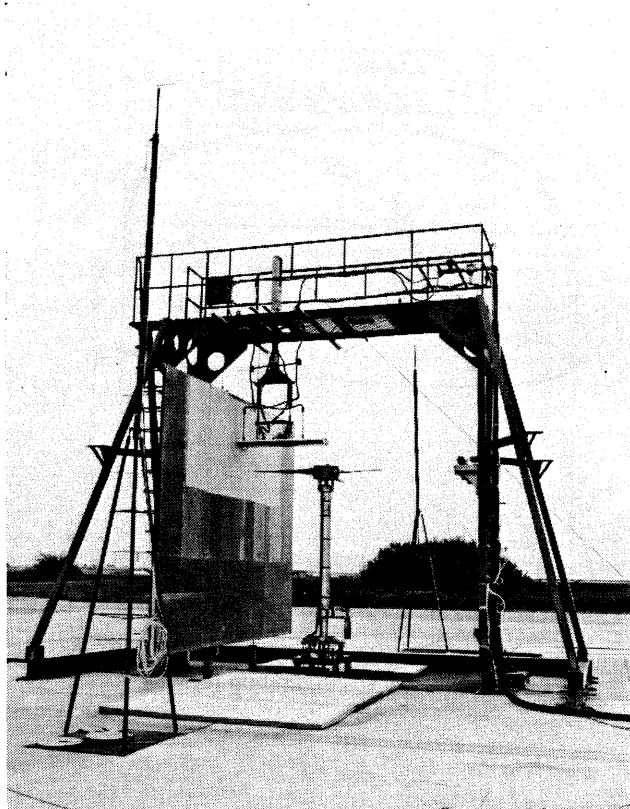
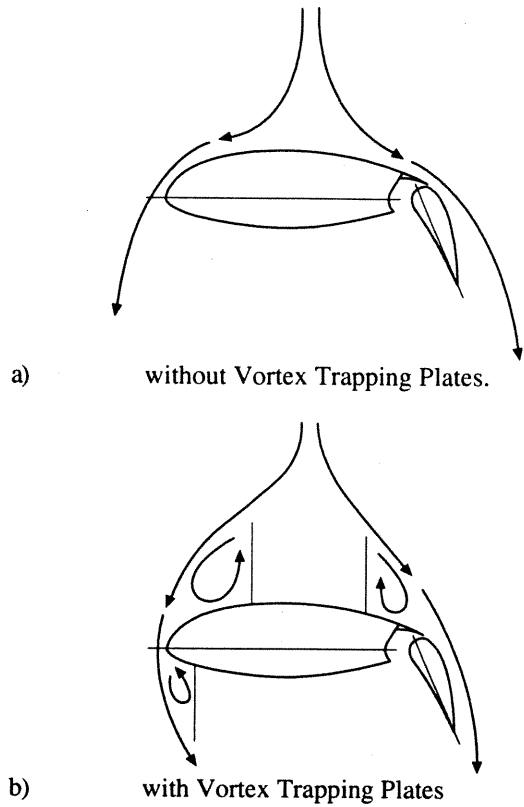


Figure 3. Installation of Hover Test Rig and Wing.

Figure 1. Flowfield around a wing at -90 deg angle of attack

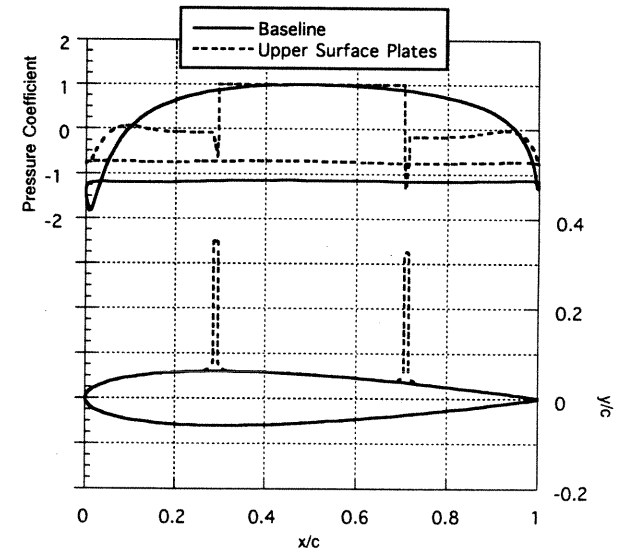


Figure 4. Predicted surface pressure for NACA 0012 baseline and Configuration (a).

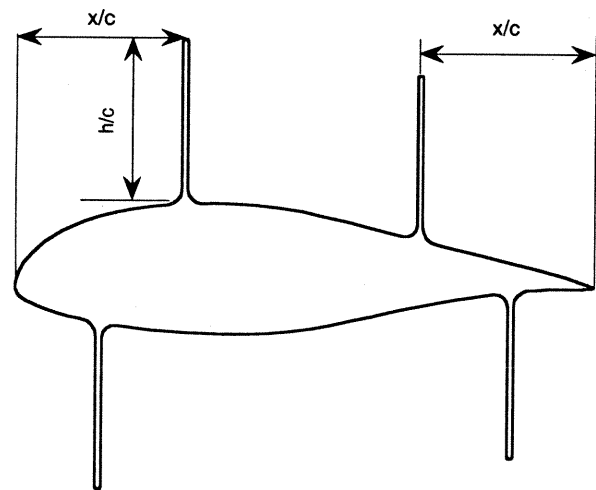


Figure 2. Plate height and offset distance for VTP configurations.

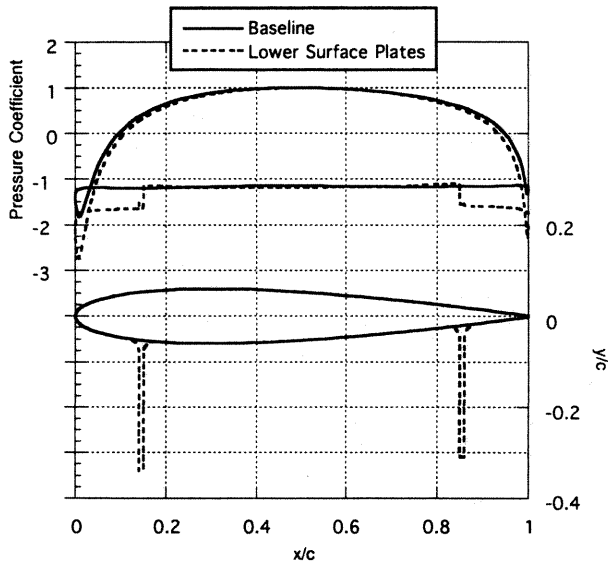


Figure 5. Predicted surface pressure for NACA 0012 baseline and Configuration (b).

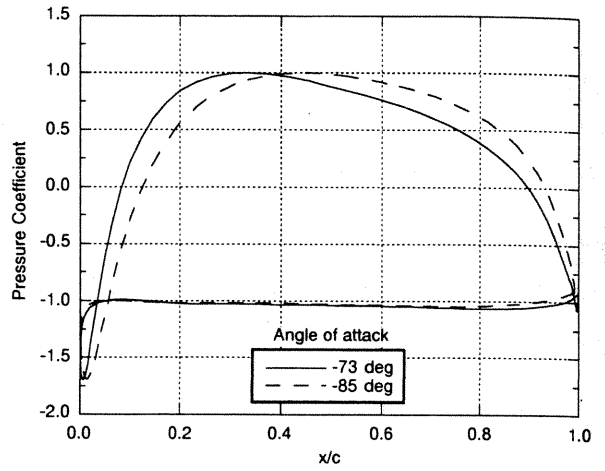


Figure 7. Predicted surface pressures for V-22 wing with different angles of attack.

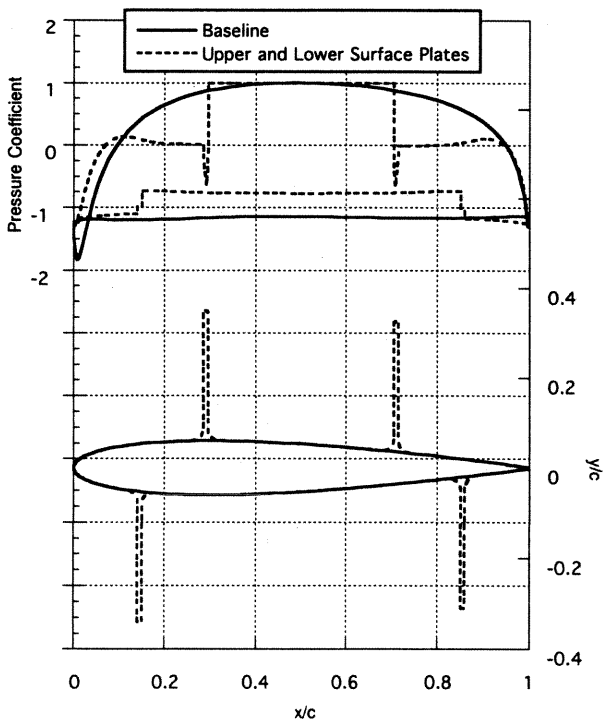


Figure 6. Predicted surface pressure for NACA 0012 baseline and Configuration (c).

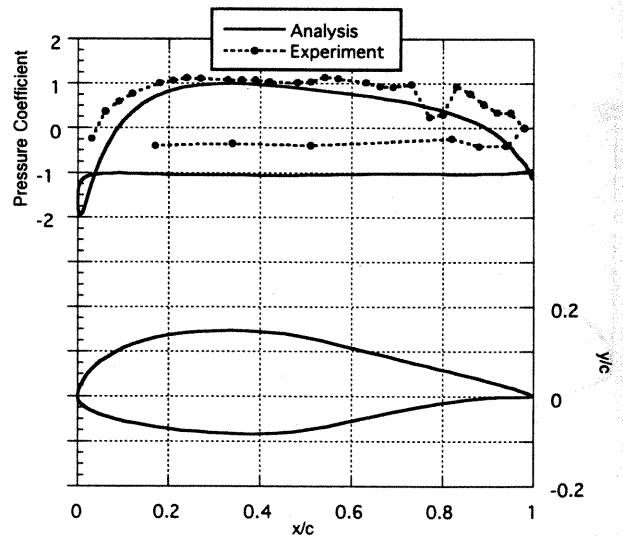


Figure 8. Predicted and measured surface pressure for the baseline V-22 wing section; flap = 0 deg.

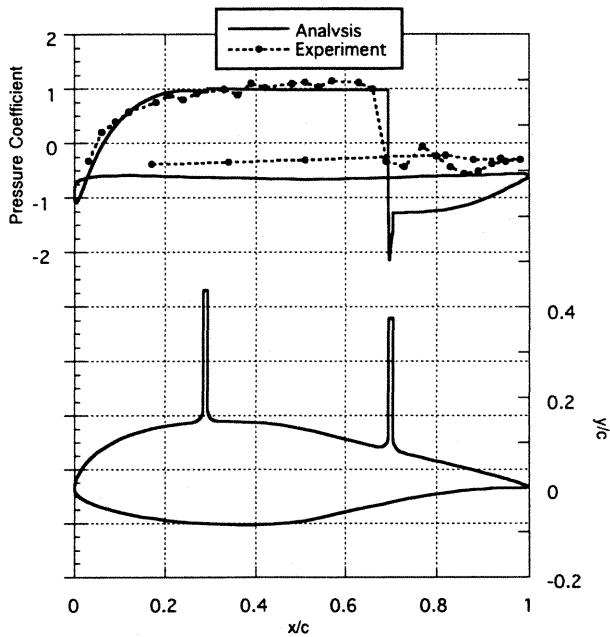


Figure 9. Predicted and measured surface pressure for Configuration (d); flap = 0 deg.

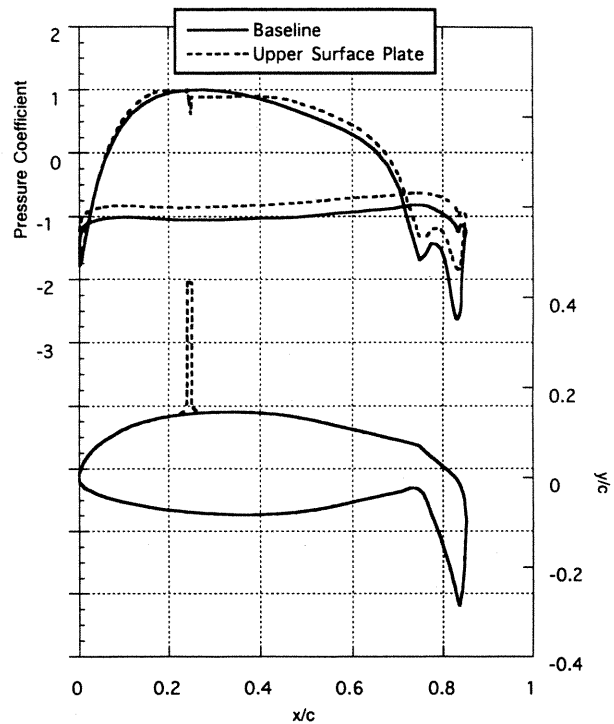


Figure 11. Predicted surface pressure for the baseline V-22 wing section and Configuration (f); flap = 78 deg.

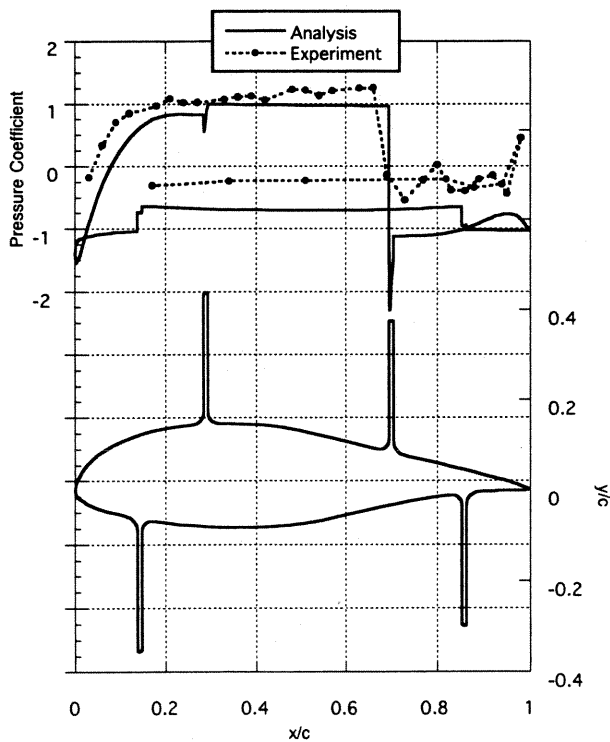


Figure 10 Predicted and measured surface pressure for Configuration (e); flap = 0 deg.

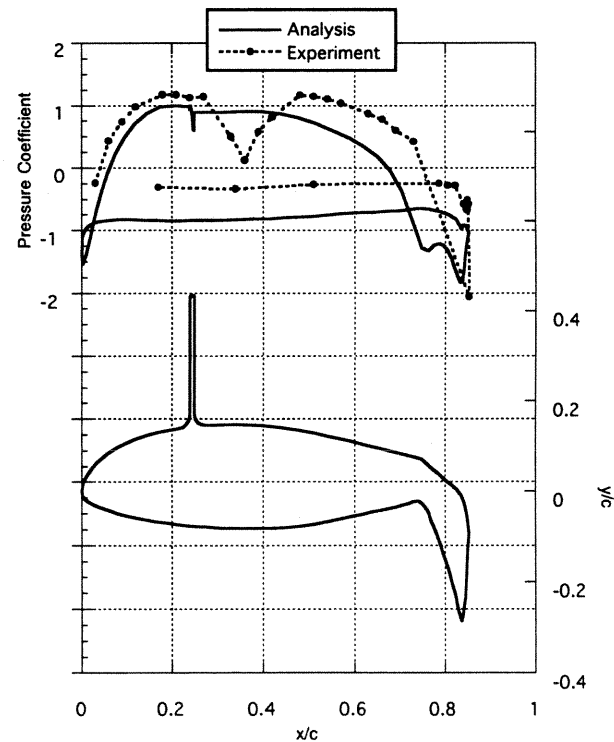


Figure 12. Predicted and measured surface pressure for Configuration (f); flap = 78 deg.

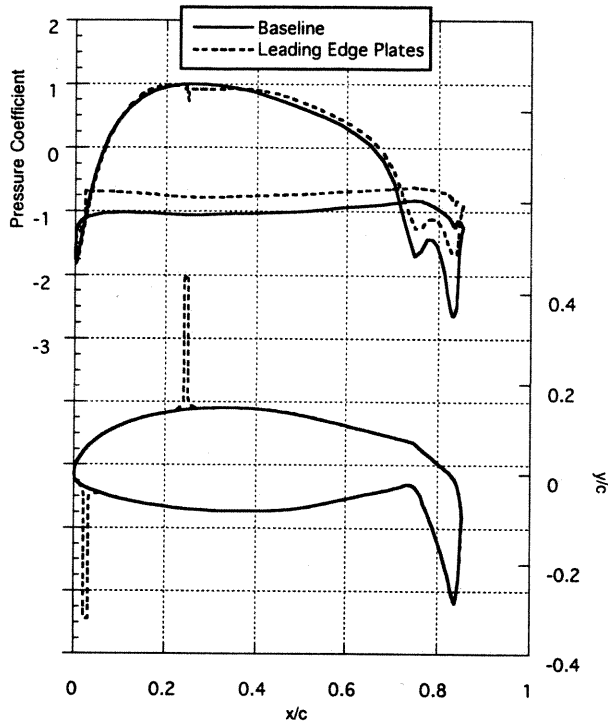


Figure 13. Predicted surface pressure for the baseline V-22 wing section and Configuration (g); flap = 78 deg.

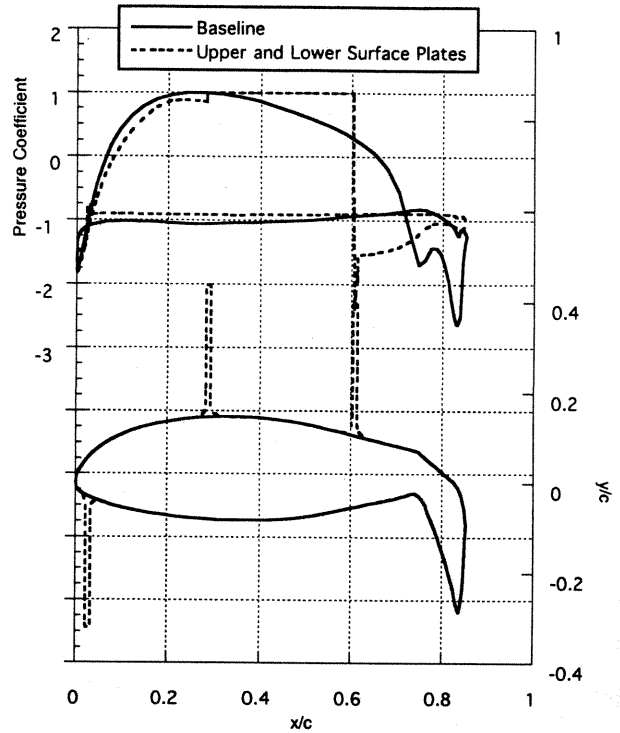


Figure 15. Predicted surface pressure for the baseline V-22 wing section and Configuration (h); flap = 78 deg.

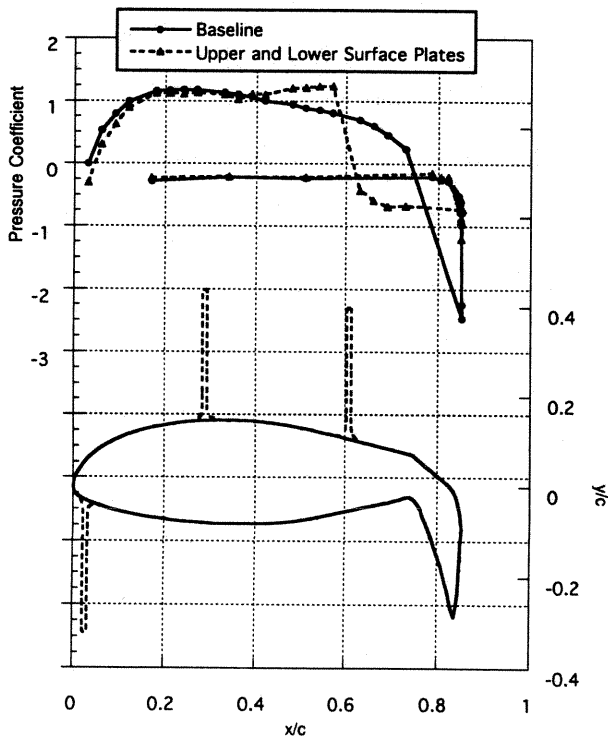


Figure 14. Measured surface pressure for the baseline V-22 wing section and Configuration (h); flap = 78 deg.

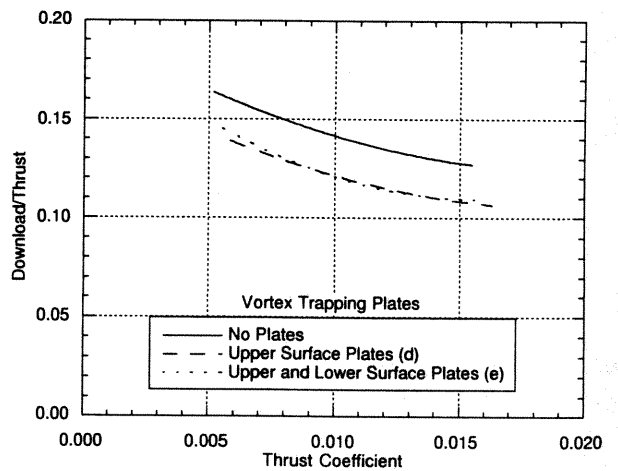


Figure 16. Effect of thrust coefficient on V-22 wing download; flap = 0 deg.

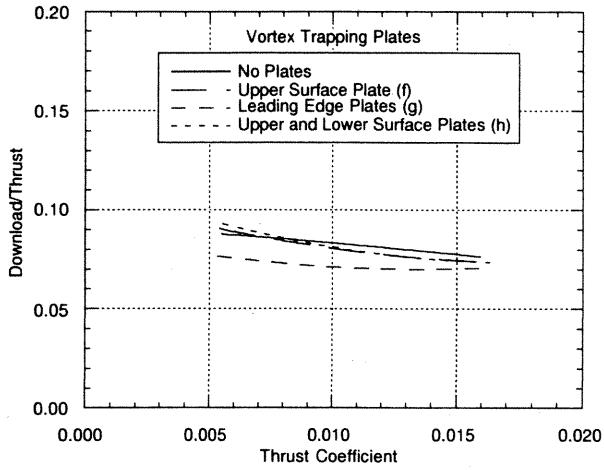


Figure 17. Effect of thrust coefficient on V-22 wing download; flap = 78 deg.

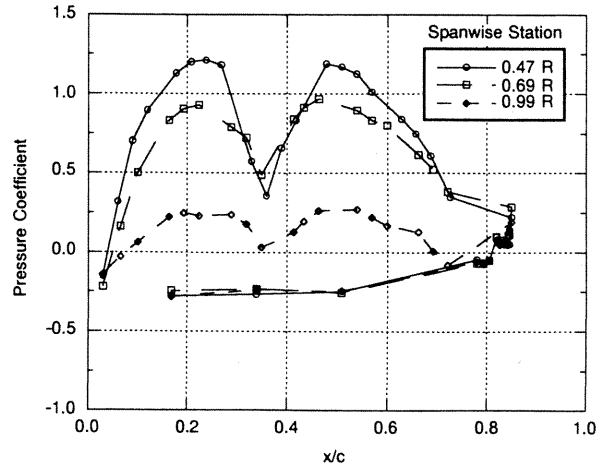


Figure 19. Spanwise vertical pressure distribution for Configuration (g).

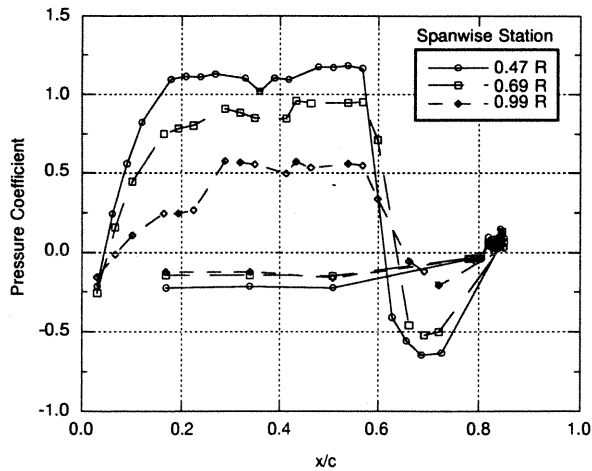


Figure 18. Spanwise vertical pressure distribution for Configuration (h).